Preprints of the 21st IFAC World Congress (Virtual)
Berlin, Germany, July 12-17, 2020

A geometric description of the set of stabilizing PID controllers

Keqin Gu * **Qian Ma** ** **Huiqing Zhou** *** **Salma Mahzoon** ****
Xingzi Yang †

* *Department of Mechanical and Industrial Engineering, Southern Illinois University Edwardsville, Edwardsville, IL 62025, USA (e-mail: kgu@siue.edu;nchoube@siue.edu)*
** *School of Automation, Nanjing University of Science and Technology, Nanjing, Jiangsu 210094, China (e-mail: qianmashine@gmail.com)*
*** *Department of Mathematics and Statistics, Southern Illinois University Edwardsville, Edwardsville, IL 62025, USA (e-mail: kgu@siue.edu;nchoube@siue.edu)*
**** *University of Oklahoma, Norman, OK 73019, USA (e-mail: salma.mahzoon@gmail.com)*
† *Department of Mechanical Engineering, University of Texas at San Antonio, San Antonio, TX 78249, USA (e-mail: xingzi.yang@utsa.edu)*

Abstract: This article presents a geometric description of the set of stabilizing PID controllers. The three-dimensional parameter space is partitioned by the stability crossing surface into regions such that the number of characteristic roots on the right half-plane (RHP) remains constant within each region. The set of stabilizing PID parameters consists those regions with no RHP root. The stability crossing surface is a ruled surface, and it is completely determined by a curve known as the discriminant. The discriminant may be divided into sectors between its cusps, and each sector corresponds to a positive patch and negative patch. The stability crossing surface is composed of these patches.

Keywords: Stability, PID control, geometric characterization.

1. INTRODUCTION

As PID control is widely used in industrial applications, it is natural that a substantial amount of research has been conducted on the selection of PID controller gains, Bazanella et al. (2017), Meza et al. (2012) are some examples.

It is valuable to identify the set of all PID gains that stabilizes the system. The first description of such stabilizing set has been achieved using the Hermite-Biehler theorem (Ho et al. (1996)). A linear programing method may be used to facilitate identifying the stabilizing set (Ho et al. (1997)). Singular frequency concept was introduced in Ackermann and Kaesbauer (2003), and a more explicit description has been achieved for a second order system in Wang (2007). To summarize, the methods in most currently available literature try to visualize the stabilizing set through its cross-section with a constant proportional gain. While such cross sections have a very simple geometric structure of polygons, it is not easy to obtain a global view of the entire stabilizing set.

In this article, we present a more natural description of the geometric structure of the stabilizing set. With the proportional gain as the vertical axis in the three-dimensional parameter space, we visualize the set by projecting it to the horizontal plane. This bird-eye view allows us to see directly all the regions in the horizontal plane where there exist proportional gains to stabilize the system. Roughly speaking, the stability crossing surface, which consists of the parameters such that at least one characteristic root is on the imaginary axis, is described. This stability crossing surface partitions the three-dimensional parameter space into regions of constant number of RHP characteristic roots. Especially, the regions where there is no RHP characteristic root form the set of stabilizing PID parameters.

2. STABILITY CROSSING SURFACE

For a given plant with transfer function $G_p(s)$, we want to determine the set of coefficients (k_d, k_i, k_p) of PID controller

$$G_c(s) = k_p + \frac{k_i}{s} + k_d s, \tag{1}$$

such that the closed-loop system is stable, i.e., all the solutions of the system characteristic equation

$$\Delta(s) = 1 + G_c(s)G_p(s) = 0 \tag{2}$$

are on the left half-plane (LHP). The study here is based on the D-decomposition method (El'Sgol'ts and Norkin (1973); Gu and Naghnaeian (2011)). Specifically, the roots

of (2) change continuously as the PID parameters change. Therefore, the number of roots on the RHP may change only when one or more roots reach the imaginary axis. For this purpose, it is instrumental to introduce the following concept of stability crossing surface.

Definition 1. The set of all $(k_d, k_i, k_p) \in \mathbb{R}^3$ such that the characteristic equation $\Delta(s) = 0$ has at least one solution on the imaginary axis is known as the *stability crossing surface*, and is denoted as $\mathcal{K}$.

In order to focus on the main idea, we make the following assumption about the plant transfer function.

Assumption 1. The transfer function can be written as $G_p(s) = N_p(s)/D_p(s)$, where $N_p(s)$ and $D_p(s)$ are polynomials with real coefficients. Furthermore, neither $N_p(s)$ nor $D_p(s)$ has any roots on the imaginary axis.

Under Assumption 1, we may set $s = j\omega$ in (2) and multiply by $\frac{j\omega}{G_p(j\omega)}$ to obtain

$$\delta(j\omega) = \frac{j\omega}{G_p(j\omega)} + j\omega k_p + k_i - \omega^2 k_d = 0. \tag{3}$$

Therefore, the stability crossing surface $\mathcal{K}$ also corresponds to the set of real solution of (3) for ω.

Let the k_p-axis be the vertical axis in the (k_d, k_i, k_p) parameter space. Then, For $\omega = 0$, we obtain from (3)

$$k_i = 0, \tag{4}$$

which is a vertical plane denoted as $\mathcal{V}$. For a fixed $\omega \neq 0$, (3) yields the following parametric equations

$$k_i = \omega^2 k_d - a(\omega), \tag{5}$$

$$k_p = -\frac{b(\omega)}{\omega}, \tag{6}$$

where

$$a(\omega) = \mathrm{Re}\left[\frac{j\omega}{G_p(j\omega)}\right], \tag{7}$$

$$b(\omega) = \mathrm{Im}\left[\frac{j\omega}{G_p(j\omega)}\right]. \tag{8}$$

Equations (5)-(8) define a horizontal straight line $\mathcal{L}(\omega)$ in $\mathbb{R}^3$,

$$\mathcal{L}(\omega) := \{(k_d, k_i, k_p) \in \mathbb{R}^3 : k_i = \omega^2 k_d - a(\omega), \\ k_p = -b(\omega)/\omega\}.$$

The projection of this straight line on the (k_d, k_i) plane is described by (5), and is denoted as $\mathcal{PL}(\omega)$. Obviously, the slope of $\mathcal{PL}(\omega)$ is ω^2.

As the plant transfer function satisfies

$$G_p(j\omega) = G_p^*(-j\omega),$$

it is obvious that $a(\omega)$ is an even function of ω, and $b(\omega)$ is an odd function of ω. Therefore, $\mathcal{L}(\omega) = \mathcal{L}(-\omega)$. It is thus sufficient to restrict ω to $(0, \infty)$.

As ω varies from 0^+ to $+\infty$, the straight lines $\mathcal{L}(\omega)$ described by (5) and (6) form a surface, which we denote as $\mathcal{S}$,

$$\mathcal{S} = \bigcup_{\omega > 0} \mathcal{L}(\omega). \tag{9}$$

Such a surface is known as a ruled surface (Guggenheimer (1997)). The surface $\mathcal{S}$ may be parameterized by k_d and ω. The stability crossing surface $\mathcal{K}$ consists of $\mathcal{S}$ and the vertical plane $\mathcal{V}$. As the parameter (k_d, k_i, k_p) crosses $\mathcal{S}$ at a point on $\mathcal{L}(\omega)$ for some $\omega \neq 0$, a pair of characteristic roots touch the imaginary axis at $\pm\omega$, and either cross it or return to the same side. If the parameter crosses the vertical surface $\mathcal{V}$, then one characteristic root crosses the imaginary axis at the origin.

As the vertical plane $\mathcal{V}$ is rather simple, we will spend most effort in understanding $\mathcal{S}$. Using the vector notation, a point in the parameter space may be expressed as

$$\mathbf{r} = k_d \mathbf{i} + k_i \mathbf{j} + k_p \mathbf{k}.$$

Then

$$(k_d, \omega) \to \mathbf{r}_{\mathcal{S}}(k_d, \omega)$$

is a parametrization of the surface $\mathcal{S} \subset \mathbb{R}^3$. Therefore, $\mathcal{S}$ can be written as

$$\mathbf{r} = \mathbf{r}_{\mathcal{S}}(k_d, \omega), \tag{10}$$

with the components as functions of k_d and ω given by (5)-(6). We will use the following plant transfer function, which was analyzed in Ackermann and Kaesbauer (2003), to illustrate our description of $\mathcal{S}$ and stability analysis in the remaining part of this article

$$G_p(s) = \frac{-s^4 - 7s^3 - 2s + 1}{(s+1)(s+2)(s+3)(s+4)(s^2+s+1)}. \tag{11}$$

3. DISCRIMINANT

Definition 2. The discriminant of the ruled surface $\mathcal{S}$ described by (5) and (6) is a curve formed by the points on $\mathcal{S}$ with vertical tangent planes.

We will use $\mathcal{D}$ to denote the discriminant. With $\mathcal{S}$ described by (10), $\frac{\partial \mathbf{r}_{\mathcal{S}}}{\partial k_d}$ and $\frac{\partial \mathbf{r}_{\mathcal{S}}}{\partial \omega}$ are the two tangents of the curves formed by fixing either ω or k_d, respectively. The cross product of $\frac{\partial \mathbf{r}_{\mathcal{S}}}{\partial k_d}$ and $\frac{\partial \mathbf{r}_{\mathcal{S}}}{\partial \omega}$ is the normal vector to $\mathcal{S}$. Therefore, a point on $\mathcal{S}$ has vertical tangent plane if and only if it satisfies

$$\left(\frac{\partial \mathbf{r}_{\mathcal{S}}}{\partial k_d} \times \frac{\partial \mathbf{r}_{\mathcal{S}}}{\partial \omega}\right) \cdot \mathbf{k} = 0, \tag{12}$$

where $\times$ is the cross product. Using the component expression, the above reduces to

$$\left(\frac{\partial k_i}{\partial \omega}\mathbf{k} - \frac{\partial k_p}{\partial \omega}\mathbf{j}\right) \cdot \mathbf{k} = 0. \tag{13}$$

Using (5) in the above equation yields

$$2\omega k_d - a'(\omega) = 0, \tag{14}$$

which can be solved for k_d to obtain

$$k_d = \frac{a'(\omega)}{2\omega}. \tag{15}$$

A substitution of (5) by (15) yields

$$k_i = \frac{1}{2}\omega a'(\omega) - a(\omega). \tag{16}$$

Therefore, the discriminant $\mathcal{D}$ is a curve that can be expressed as

$$k_d = k_d^d(\omega) = \frac{a'(\omega)}{2\omega}, \tag{17}$$

$$k_i = k_i^d(\omega) = \frac{1}{2}\omega a'(\omega) - a(\omega), \tag{18}$$

$$k_p = k_p^d(\omega) = -\frac{b(\omega)}{\omega}. \tag{19}$$

The discriminant of the system with plant transfer function (11) is shown in Fig. 1.

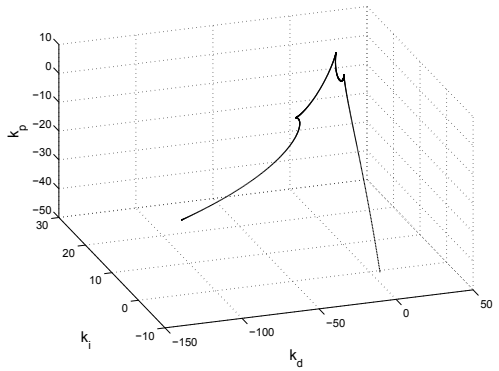

Fig. 1. Discriminant of the ruled surface of system (11).

It is instrumental to represent discriminant $\mathcal{D}$ by its projection to the horizontal plane and its vertical component as a function of ω. The horizontal projection is denoted as $\mathcal{PD}$, and is described by (17) and (18). For the system with plant transfer function (11), $\mathcal{PD}$ is plotted in Fig. 2.

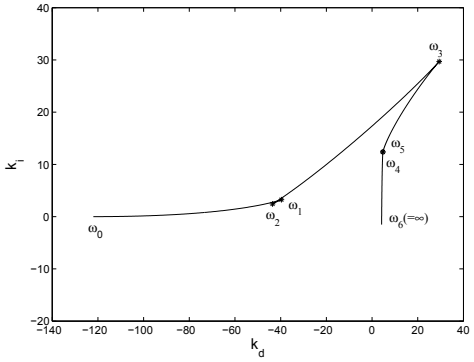

Fig. 2. The projection of discriminant $\mathcal{PD}$ with cusps ω_i.

A critical observation is that $\mathcal{PD}$ is the envelope of the family of straight lines $\mathcal{PL}(\omega)$. This can be shown as follows. Define $\phi(\omega) = \omega a'' - a'(\omega)$. Taking the derivative of (17) and (18), we obtain

$$(k_d^d)'(\omega) = \frac{\omega a'' - a'(\omega)}{2\omega^2} = \frac{\phi(\omega)}{2\omega^2}, \tag{20}$$

$$(k_i^d)'(\omega) = \frac{\omega a'' - a'(\omega)}{2} = \frac{\phi(\omega)}{2}. \tag{21}$$

When

$$\phi(\omega) \neq 0, \tag{22}$$

the slope of the tangent of $\mathcal{PD}$ at ω is ω^2, which is identical to $\mathcal{PL}(\omega)$. It is also obvious that $k_d^d(\omega)$ and $k_i^d(\omega)$ satisfies (5), which indicates that this point in $\mathcal{PD}$ belongs to the straight line $\mathcal{PL}(\omega)$. This allows us to conclude that the tangent of $\mathcal{PD}$ at ω indeed coincides with $\mathcal{PL}(\omega)$, which is formally stated in the following theorem.

Theorem 1. The surface $\mathcal{S}$ is completely determined by the discriminant $\mathcal{D}$.

Indeed, as $\mathcal{D}$ is given by (17), (18) and (19), it is necessary that

$$(k_i^d)'(\omega) = \omega^2 (k_d^d)'(\omega), \tag{23}$$

and $\mathcal{S}$ can be expressed as

$$k_d = k_d^d(\omega) + \gamma, \tag{24}$$

$$k_i = k_i^d(\omega) + \omega^2\gamma, \tag{25}$$

$$k_p = k_p^d(\omega), \tag{26}$$

with $\omega \in (0, \infty)$ and $\gamma \in (-\infty, \infty)$.

For a fixed ω, (24), (25) and (26) represent $\mathcal{L}(\omega)$ since (24)-(25) satisfy (5). It is useful to divide $\mathcal{L}(\omega)$ at the point $\mathbf{r}^d(\omega) = (k_d^d(\omega), k_i^d(\omega), k_p^d(\omega))$ into two parts

$$\mathcal{L}^+(\omega) = \{(k_d^d(\omega) + \gamma, k_i^d(\omega) + \omega^2\gamma, k_p^d(\omega)) \mid \gamma > 0\},$$

$$\mathcal{L}^-(\omega) = \{(k_d^d(\omega) + \gamma, k_i^d(\omega) + \omega^2\gamma, k_p^d(\omega)) \mid \gamma < 0\}.$$

Naturally, their projections on the (k_d, k_i) plane are denoted as $\mathcal{PL}^+(\omega)$ and $\mathcal{PL}^-(\omega)$, respectively.

4. CUSPS AND PATCHES

Assumption 2. No $\omega \in (0, \infty)$ may simultaneously satisfy

$$\phi(\omega) = \omega a''(\omega) - a'(\omega) = 0, \tag{27}$$

$$\phi'(\omega) = \omega a'''(\omega) = 0. \tag{28}$$

If $\omega = \omega^*$ violates (22), i.e., $\phi(\omega^*) = 0$, then the above assumption means that $\phi(\omega)$ must have opposite signs for $\omega = \omega^* + \varepsilon$ and $\omega = \omega^* - \varepsilon$ when $\varepsilon > 0$ is sufficiently small, and $(k_d^d(\omega^*), k_i^d(\omega^*))$ is a cusp of $\mathcal{PD}$. This is obvious if we notice that $k_d^{d'}(\omega)$ and $k_i^{d'}(\omega)$ change sign at such a point. At a cusp, the tangent to $\mathcal{PD}$ may still be defined by its limit, and still has the slope ω^2. The tangent of the discriminant $\mathcal{D}$ at such a point is vertical if

$$\frac{dk_p^d}{d\omega} = \left[-\frac{b(\omega)}{\omega}\right]' \neq 0. \tag{29}$$

It is not too difficult to handle degenerate points that violate Assumption 2. For instance, let $\phi^{(k)}(\omega) = 0$ for $k = 0, 1, \ldots, m-1$, and $\phi^{(m)}(\omega) \neq 0$, then ω corresponds to a cusp if m is odd, but it is not a cusp if m is even, and the readers should not have difficulty generalizing the analysis in this article to such cases.

For the system with plant transfer function (11), $\mathcal{PD}$ has five cusps, and the corresponding ω are denoted as ω_i, $i = 1, 2, \ldots 5$. These cusps are also labeled in Fig. 2.

Let ω_i, $i = 1, 2, \ldots, n-1$ correspond to the cusps of $\mathcal{PD}$, and be arranged in ascending order

$$\omega_1 < \omega_2 < \cdots < \omega_{n-1}.$$

They partition $(0, \infty)$ into n intervals Ω_i, $i = 1, 2, \ldots, n$,

$$\begin{aligned}\Omega_1 &= (0, \omega_1],\\ \Omega_i &= [\omega_{i-1}, \omega_i],\ i = 2, 3, \ldots, n-1,\\ \Omega_n &= [\omega_{n-1}, \infty).\end{aligned}$$

Correspondingly, we may partition the discriminant $\mathcal{D}$ into n sectors

$$\mathcal{D}_i = \{(k_d^d(\omega), k_i^d(\omega), k_p^d(\omega)) | \omega \in \Omega_i\}.$$

The projection of $\mathcal{D}_i$ on the (k_d, k_i) plane is denoted as $\mathcal{PD}_i$. Obviously, $\mathcal{PD}_i$, $i = 1, 2, \ldots, n$, partition $\mathcal{PD}$.

It is observed that the slope of $\mathcal{PD}_i$ is ω^2, which increases as one moves along $\mathcal{PD}_i$ along the directions of increasing ω, from which we may use the Theorem on Turning Tangent (Chern (1967)) to arrive at the following theorem.

Theorem 2. The center of curvature is always on the left hand side as one traverses $\mathcal{PD}_i$ along the direction of increasing ω. The region bounded by $\mathcal{PD}_i$ and the line segment connecting the two end points of $\mathcal{PD}_i$ is convex.

We may also partition $\mathcal{S}$ into $2n$ patches

$$\mathcal{S}_i^+ = \bigcup_{\omega \in \Omega_i} \mathcal{L}^+(\omega), \mathcal{S}_i^- = \bigcup_{\omega \in \Omega_i} \mathcal{L}^-(\omega).$$

$\mathcal{S}_i^+$ is referred to as the ith positive patch, and $\mathcal{S}_i^-$ the ith negative patch. Their projections on the (k_d, k_i) plane are denoted as $\mathcal{PS}_i^+$ and $\mathcal{PS}_i^-$, respectively. Obviously,

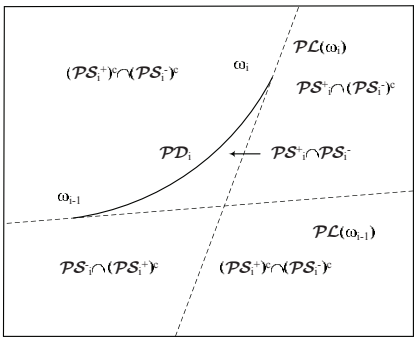

Fig. 3. Division with $\mathcal{PD}_i$, $\mathcal{PL}(\omega_{i-1})$, and $\mathcal{PL}(\omega_i)$.

$\mathcal{D}_i$, $\mathcal{L}^+(\omega_{i-1})$ and $\mathcal{L}^+(\omega_i)$ form the boundary of $\mathcal{S}_i^+$, and $\mathcal{D}_i$, $\mathcal{L}^-(\omega_{i-1})$ and $\mathcal{L}^-(\omega_i)$ form the boundary of $\mathcal{S}_i^-$. $\mathcal{PD}_i$, $\mathcal{PL}(\omega_{i-1})$ and $\mathcal{PL}(\omega_i)$ divide $\mathbb{R}^2$ into five regions as shown in Fig. 3, $\mathcal{PS}_i^+ \cap (\mathcal{PS}_i^-)^c$, $\mathcal{PS}_i^+ \cap \mathcal{PS}_i^-$, $(\mathcal{PS}_i^+)^c \cap \mathcal{PS}_i^-$, and two components of $(\mathcal{PS}_i^+)^c \cap (\mathcal{PS}_i^-)^c$.

$\mathcal{PD}_i$, $i = 1, 2, \ldots, n$; $\mathcal{PL}^{\pm}(0)$, $\mathcal{PL}^{\pm}(\omega_i)$, $i = 1, 2, \ldots, n-1$, and possibly $\mathcal{PL}^{\pm}(\infty)$ when applicable, partition the (k_d, k_i) plane into open regions. Denote these regions as R_k, $k = 1, 2, \ldots, N$,

$$\mathrm{cl}\left(\bigcup_{k=1}^{N} R_k\right) = \mathbb{R}^2,\ R_k \cap R_l = \emptyset,$$

where cl is the closure operator on a set. Consider a given region R_k. As it does not contain the boundary of $\mathcal{PS}_i^+$ or $\mathcal{PS}_j^-$, we may associate R_k with a pair of index sets $\mathcal{I}_k^+ \subset \mathbb{N}_n$, $\mathcal{I}_k^- \subset \mathbb{N}_n$, where $\mathbb{N}_n = \{1, 2, \ldots, N\}$. For each point $\mathbf{r} = (k_d, k_i) \in R_k$, $\mathbf{r} \in \mathcal{PS}_i^+$ or $\mathbf{r} \in \mathcal{PS}_j^-$ if and only if $i \in \mathcal{I}_k^+$ or $j \in \mathcal{I}_k^-$, respectively.

Let $\mathcal{I}_k^+ = \{i_1, i_2, \ldots, i_l\}$, $\mathcal{I}_k^- = \{j_1, j_2, \ldots, j_m\}$, and represent these two index sets by a single set

$$\mathcal{I}_k = \left\{i_1^+, i_2^+, \ldots, i_l^+, j_1^-, j_2^-, \ldots, j_m^-\right\} \subset \mathbb{N}_n^{\pm}, \quad (30)$$

where $\mathbb{N}_n^{\pm} = \{1^+, 2^+, \ldots, n^+, 1^-, 2^-, \ldots, n^-\}$. Such a notation also allows us to use the same notation $\mathcal{S}_\alpha$ to represent positive and negative patches,

$$\mathcal{S}_\alpha = \begin{cases} \mathcal{S}_i^+ \text{ if } \alpha = i^+, \\ \mathcal{S}_j^- \text{ if } \alpha = j^-. \end{cases}$$

The same can be done for $\mathcal{PS}_i^+$ and $\mathcal{PS}_i^-$. Then the above can be summarized in the following theorem.

Theorem 3. For $\mathcal{I}_k$ defined above, one has

$$\begin{aligned}&R_k \subset \mathcal{PS}_\alpha,\ \alpha \in \mathcal{I}_k,\\ &R_k \cap \mathcal{PS}_\alpha = \emptyset,\ \alpha \notin \mathcal{I}_k,\\ &R_k \subset \left(\bigcap_{\alpha \in \mathcal{I}_k} \mathcal{PS}_\alpha\right) \cap \left(\bigcup_{\beta \in \mathbb{N}_n^{\pm} \setminus \mathcal{I}_k} (\mathcal{PS}_\beta)^c\right).\end{aligned}$$

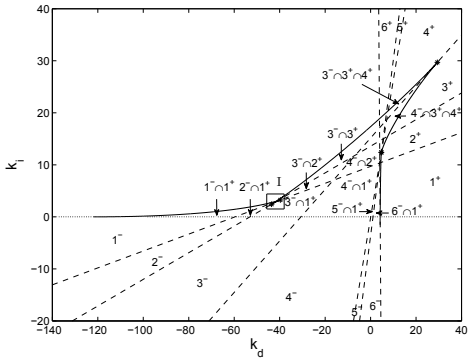

Fig. 4. The regions (based on Fig. 2).

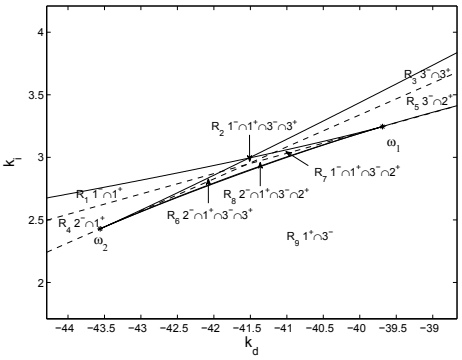

Fig. 5. Region I, which is identified with a box in Fig. 4.

For the system with plant transfer function (11), the partition of the (k_d, k_i) plane with the corresponding index

sets is given in Fig. 4 with amplified view of region I given in Figs. 5. In the figures, a region R_k with index set $\mathcal{I}_k$ given in (30) is labeled as $i_1^+ \cap i_2^+ \cap \ldots \cap i_l^+ \cap j_1^- \cap j_2^- \cap \ldots \cap j_m^-$. Given any point $(k_d^*, k_i^*) \in R_k$, the vertical

$$\mathcal{VL}(k_d^*, k_i^*) = \{(k_d^*, k_i^*, k_p) | -\infty < k_p < \infty\}$$

intersects with all patches $\mathcal{S}_\alpha$, $\alpha \in \mathcal{I}_k$, but does not intersect with any patch $\mathcal{S}_\beta$, $\beta \notin \mathcal{I}_k$.

5. RELATIVE VERTICAL POSITIONS OF PATCHES

For a given point $(k_d, k_i) \in R_k$, let the intersection of $\mathcal{VL}(k_d, k_i)$ and $\mathcal{S}_\alpha$ be $(k_d, k_i, k_{p\alpha})$. Assume

$$k_{p\alpha} \neq k_{p\beta}, \ \textit{whenever} \ \alpha \neq \beta. \tag{31}$$

Then, we can order the elements of the index set $\mathcal{I}_k$ as $\alpha_1, \alpha_2, \ldots, \alpha_{l+m}$, such that

$$k_{p\alpha_1} > k_{p\alpha_2} > \cdots > k_{p\alpha_{l+m}}.$$

In this case, we write, at (k_d, k_i),

$$\mathcal{S}_{\alpha_1} > \mathcal{S}_{\alpha_2} > \cdots > \mathcal{S}_{\alpha_{l+m}}. \tag{32}$$

In general, the order is different for different $(k_d, k_i) \in R_k$.

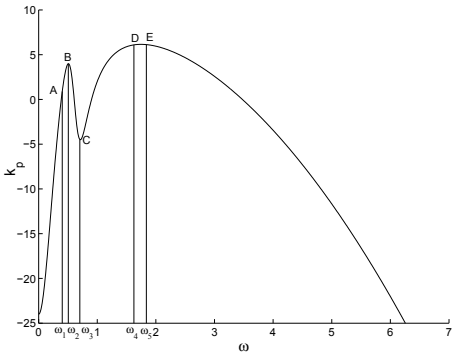

Fig. 6. The change of k_p with ω.

For a complete stability analysis, we want to further partition R_k into subregions R_{ki}, $i = 1, 2, \ldots, m_k$, such that the order (32) is independent of (k_d, k_i) as long as it is within the subregion R_{ki}. The internal boundaries that divide R_k into these subregions are the intersections between the patches projected on the (k_d, k_i) plane. Such boundaries consist of points in the (k_d, k_i) plane that violate (31), and can be obtained by considering the k_p vs ω relation. For the plant transfer function given by (11), the relation is given in Fig. 6. Let $\omega_a \neq \omega_b$, satisfy

$$k_p(\omega_a) = k_p(\omega_b), \tag{33}$$

Then $\mathcal{L}(\omega_a)$ intersects $\mathcal{L}(\omega_b)$. The collection of all (ω_a, ω_b) that satisfy (33) corresponds to all the intersections between different patches. Within each R_{ki}, we may order the index set $\mathcal{I}_k$ such that (32) is true for all $(k_d, k_i) \in R_{ki}$. (32) may be interpreted as $\mathcal{S}_{\alpha_1}$ above $\mathcal{S}_{\alpha_2}$, which in turn is above $\mathcal{S}_{\alpha_3}$, and so on. Within the column $\bigcup \{\mathcal{VL}(k_d, k_i) | (k_d, k_i) \in R_{ki}\}$, for any (k_d, k_i, k_p) in the region between $\mathcal{S}_{\alpha_j}$ and $\mathcal{S}_{\alpha_{j+1}}$, the characteristic equation has a fixed number of roots on the RHP. This is also true for the region above $\mathcal{S}_{\alpha_1}$ and below $\mathcal{S}_{\alpha_{l+m}}$.

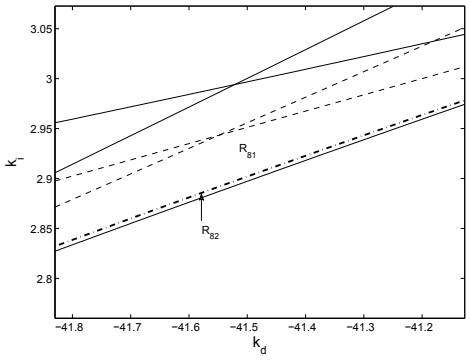

Fig. 7. In Region I, the intersection curve divides R_8 into R_{81} and R_{82}.

We now discuss how to determine the relative vertical positions of $\mathcal{S}_\alpha$, $\alpha \in \mathcal{I}_k$ within each R_{ki}. We need to only choose an arbitrary $(k_d^*, k_i^*) \in R_{ki}$ to determine this order as it does not change within R_{ki}. This can be carried out as follows: For each $\alpha \in \mathcal{I}_k$, if $\mathcal{S}_\alpha$ is a positive patch, say S_j^+, then we may determine the unique $\omega_\alpha \in (\omega_{j-1}, \omega_j)$ such that $(k_d^*, k_i^*) \in \mathcal{PL}^+(\omega_\alpha)$. If $\mathcal{S}_\alpha$ is a negative patch, then we need $(k_d^*, k_i^*) \in \mathcal{PL}^-(\omega_\alpha)$ instead. Geometrically, this means drawing a tangent of $\mathcal{PD}_i$ that passes through the point (k_d^*, k_i^*), and the point (k_d^*, k_i^*) is on the right of the tangent point if it is a positive patch, and it is on the left if it is a negative patch. ω_α can be easily determined numerically. Indeed, $\mathcal{PL}(\omega_\alpha)$ must satisfy (5) for $k_d = k_d^*$, $k_i = k_i^*$, and $\omega = \omega_\alpha$. As k_d^* and k_i^* are given, (5) may be written as a polynomial equation of ω. The applicable solution ω_α needs to be real and satisfy $\omega_\alpha \in (\omega_{j-1}, \omega_j)$ and $k_d^d(\omega_\alpha) < k_d^*$ (if $\mathcal{S}_\alpha$ is a positive patch) or $k_d^d(\omega_\alpha) > k_d^*$ (if $\mathcal{S}_\alpha$ is a negative patch). Corresponding to the $l + m$ elements of the index set $\mathcal{I}_k$, $\alpha_1, \alpha_2, \ldots, \alpha_{l+m}$, we may find $\omega_{\alpha_1}, \omega_{\alpha_2}, \ldots, \omega_{\alpha_{l+m}}$. They should be arranged in a order so that

$$k_p(\omega_{\alpha_1}) > k_p(\omega_{\alpha_1}) > \cdots > k_p(\omega_{\alpha_{l+m}}).$$

As a result, the patches satisfy

$$\mathcal{S}_{\alpha_1} > \mathcal{S}_{\alpha_2} > \cdots > \mathcal{S}_{\alpha_{l+m}},$$

in R_{ki}.

Fore R_8 shown in Fig. 5, we conclude that

$$\mathcal{S}_2^+ > \mathcal{S}_3^- > \mathcal{S}_2^- > \mathcal{S}_1^+ \quad \text{in } R_{81}, \tag{34}$$

$$\mathcal{S}_2^+ > \mathcal{S}_2^- > \mathcal{S}_3^- > \mathcal{S}_1^+ \quad \text{in } R_{82}. \tag{35}$$

And the ordering of patches of Region I is given in Fig. 8.

6. CROSSING DIRECTIONS

Theorem 4. As the parameter (k_d, k_i, k_p) moves across a positive patch along the $\mathcal{VL}(k_d, k_i)$ in the increasing k_p direction, two roots of the characteristic equation (2) cross the imaginary axis from RHP to the LHP. The crossing of the characteristic roots is in the opposite direction if it is a negative patch.

Proof. Due to the space limitation, we omit it here.

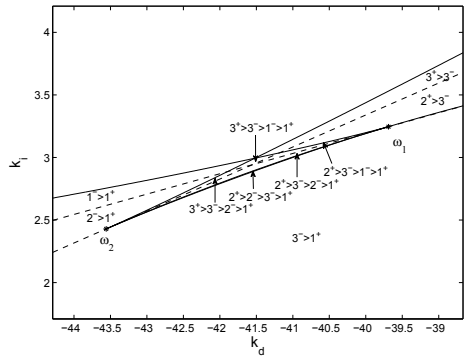

Fig. 8. The orders of the layers in Region I.

With the knowledge of the crossing direction and the vertical relative position of each region R_{ki}, we only need the number of RHP roots at one point in the parameter space to determine the number of RHP roots in each region. For one point with the known RHP roots, we can judge the crossing direction when this point crosses the surface $\mathcal{S}$ vertically. Then, the change of the number of the RHP roots is obtained. Finally, we can identify the set of stabilizing parameters.

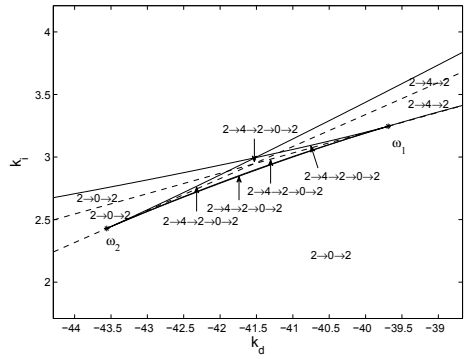

Fig. 9. The change of the roots on RHP of Region I.

For the system with plant transfer function (11), we can easily calculate that the system has two characteristic roots on the RHP when $k_i > 0$ and k_p is sufficiently large (above all the patches, $k_p > 7$ would be sufficient in view of Fig. 6). It has three RHP roots when $k_i < 0$ and k_p is large enough. The difference is due to the crossing of $\mathcal{V}$.

Now consider (k_d, k_i) in the region R_{81}. The relative vertical position of the patches is shown in (34). We already know that equation (2) has two RHP roots when (k_d, k_i, k_p) is in the region above $\mathcal{S}_2^+$. As $\mathcal{S}_2^+$ is a positive patch, we can conclude from Theorem 4 that (2) has four RHP roots when the parameters are in the region between $\mathcal{S}_3^-$ and $\mathcal{S}_2^+$ (two more than above $\mathcal{S}_2^+$ because we need to cross $\mathcal{S}_2^+$ in the negative k_p direction in order to reach from the region above $\mathcal{S}_2^+$ to this region). As $\mathcal{S}_3^-$ is a negative patch, we can similarly use Theorem 4 to determine that (2) has two RHP roots when (k_d, k_i, k_p) is in the region between $\mathcal{S}_3^-$ and $\mathcal{S}_2^-$ (two less than the region above) and (2) has no RHP root when (k_d, k_i, k_p) is between $\mathcal{S}_2^-$ and $\mathcal{S}_1^+$, and it has two RHP roots when (k_d, k_i, k_p) is below $\mathcal{S}_1^+$. This is denoted in Fig. 9 as $2 \to 4 \to 2 \to 0 \to 2$. The same process can be applied to all the regions R_{ki}. The stabilizing set is shown in the three-dimensional view in Fig. 10.

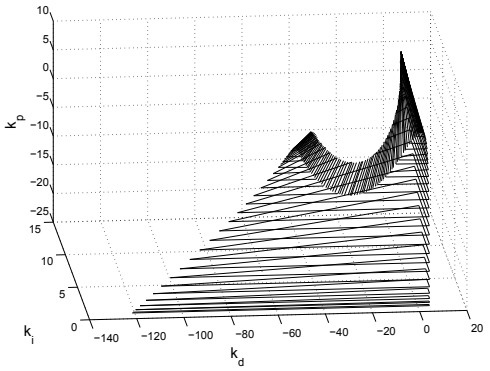

Fig. 10. The stable regions.

7. CONCLUSION

From the above discussion, it can be concluded that the set of stabilizing PID controller can be completely characterized, and a global view of the entire stabilizing set is obtained.

REFERENCES

J. Ackermann and D. Kaesbauer. Stable polyhedra in parameter space. *Automatica*, vol. 39, No. 5, pp. 937-943, 2003.

A. Bazanella, L. Pereira, and A. Parraga. A new method for PID tuning including plants without ultimate frequency. *IEEE Transactions on Control Systems Technology*, vol. 25, no. 2, pp. 637-644, 2017.

S. S. Chern (ed), *Studies in Global Geometry and Analysis*, New Jersey: Prentice-Hall, 1967.

L. L. El'Sgol'ts and S. B. Norkin. *Introduction to the Theory and Application of Differential Equations with Deviating Arguments*, Translated by J. L. Casti, Academic Press, New York, 1973.

H. Guggenheimer. *Differential Geometry*, New York, Dover, 1977.

K. Gu and M. Naghnaeian. Stability crossing set for systems with three delays. *IEEE Transactions on Automatic Control*, vol. 56, No. 1, pp. 11-26, 2011.

M. Ho, A. Datta, and S. Bhattacharyya. A new approach to feedback stabilization. In *Conference on Decision and Control*, Kobe, Japan, December, 1996.

M. Ho, A. Datta, and S. Bhattacharyya. Control system design using low order controllers: Constant gain, PI and PID. In *Proceeding of the American Control Conference*, Albuquerque, New Mexico, June, 1997.

L H. Loomis and S. Sternberg, *Advanced Calculus*, Boston, Jones and Bartlett Publishers, 1990.

J. Meza, V. Santibanez, R. Soto, and M. Llama, "Fuzzy self-tuning PID semiglobal regulator for robot manipulators," *IEEE Transactions on Industrial Electronics*, vol. 59, no. 6, pp. 2709-2717, 2012.

D. Wang. Further results on the synthesis of PID controllers. *IEEE Transactions on Automatic Control*, vol. 52, No. 6, pp. 1127-1132, 2007.